

## CIS2 Seminar Critical Review

### Introduction

For our project, we are working to develop software for a system that can perform 3D reconstruction in endoscopic applications based on a structured light approach. Both of the papers reviewed here present systems for 3D reconstruction with an endoscope and laser projected pattern with software similar to that we are working to develop. In particular, the first paper uses a uniform grid of dots (presumably white) while the second paper uses a more irregular pattern of colored dots. Both of these patterns are quite similar to our own laser pattern, indicating that techniques used in these paper may be useful to us as well, since the laser pattern itself plays a major role in what types of algorithms work best. Additionally, these papers provide general guidance on how to conduct relevant testing of 3D reconstruction algorithms.

### Paper 1: Miniaturized three-dimensional endoscopic imaging system based on active stereovision

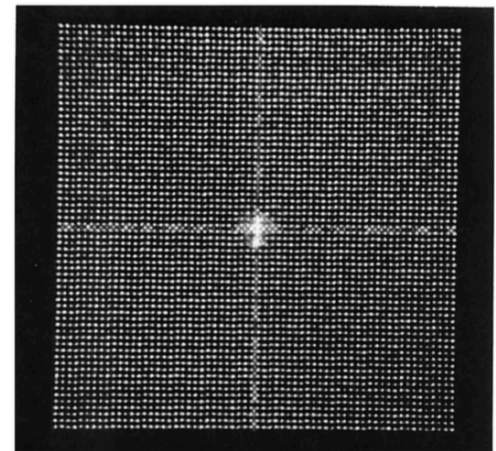
#### Motivation

Video-guided minimally invasive surgery can reduce adverse effects for patients, but is limited in that the surgeon only sees a geometrically distorted 2D image of the surgical site. It would be desirable for the surgeon to have more accurate information on the surface topology of the surgical site from a 3D imaging system as this can guide diagnosis and surgery. Since the types of feature points typically used for 3D reconstruction may be limited on human tissue, a structured light approach is ideal as the light creates feature points.

#### Technical Approach

##### *Endoscopic Imaging System*

This paper presents a system that uses a dual-channel rigid endoscope in which one channel projects the structured light pattern while the other takes the image. Shining a light source through a binary phase grating generated the structured light pattern, and a 64x64 grating was selected as this provided a larger number of sample feature points than other options (depicted to the right). However, this grating produced a “zero-order beam” at the center of the image, which is essentially a bright spot at the center of the laser pattern. In order to account for this, only a quarter of the dot matrix was used. White illumination light was turned off during collection of images for 3D reconstruction to allow for maximal contrast between laser dots and background.



(b)

##### *Calibration of the Endoscopic System*

Calibration of the imaging channel of the endoscope was performed according to a standard pinhole camera model using Tsai’s two-step calibration procedure. Using known 3D points from a checkerboard at a known distance, this calibration provided the focal length, radial distortion coefficients, scaling factor, and image center. A 3D reprojection error of less than 2.1% and visual assessment of the reprojection confirmed the success of

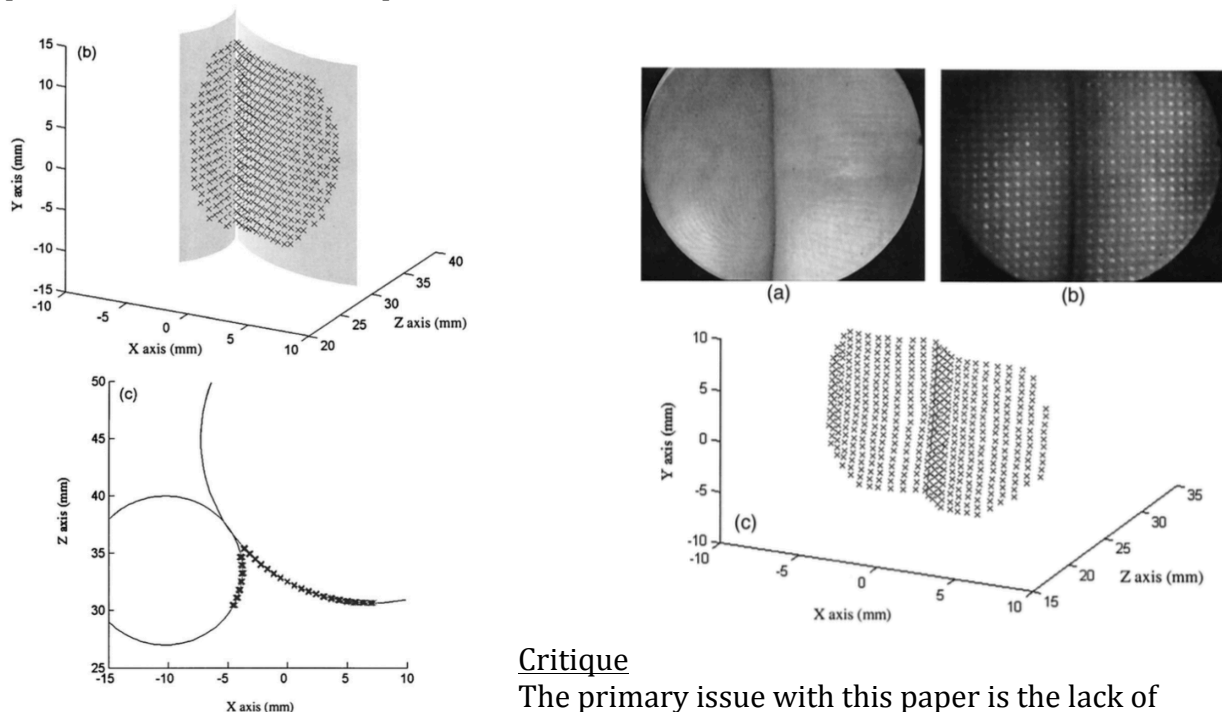
calibration. Since the projection channel is essentially the reverse of the imaging channel, these calculated parameters for the imaging channel were the same for the projection channel.

### *Three-Dimensional Measurements*

The dots in the images were extracted and labeled by first binarizing images then performing blob detection. Correspondences between dots in the image and the known pattern were established by computing a ray through the camera pinhole and the image pixel for the center of the dot in the image (based on camera calibration parameters) and computing an epipolar line in the projection channel image plane based on this ray. The dot closest to this epipolar line was considered a potential match. Potential matches were confirmed by comparison with four neighboring dots. 3D coordinates of feature points were found by intersecting the rays for the dot in the image and the dot in the projected pattern.

### Results

A one-dimensional translation stage was used to accurately control distances between the camera and imaged items. First, the paper presents results from 3D reconstruction of objects with known dimensions including a rigid plane, a step target, and a curved object made with a pair of attached cylinders. This gave percent errors of the feature points around 2-3% (results for curved object shown below). Next, results from reconstruction of forearm skin placed against a glass plate to form a flat tissue surface indicated that the accuracy was similar to that found with basic objects even though the signals of the feature points were weaker. Finally, reconstruction was performed on the finger tips and an oral cavity. Recovered sizes for the fingers were found to be consistent with approximate caliper measurements. For the oral cavity, the results generally looked correct but no quantitative evaluation was provided.



### Critique

The primary issue with this paper is the lack of quantitative results in a realistic setting. Although

good quantitative results were presented for basic objects and reconstruction of skin surfaces, no such results were presented for the more realistic oral cavity. In addition, no comments were made on the runtime of this algorithm for a given image. This is important information as the stated goal is to provide this 3D reconstruction information during surgery. Lastly, this system uses a rigid endoscope, which is not ideal for many procedures, but the authors mention that creating a similar system with a flexible endoscope is a future goal.

### Relevance

This paper suggests a workaround for the “zero-order beam” that produces a bright spot in the center of the laser pattern by using only a quarter of the pattern. Although our number of features is too limited to do this, we may consider other ways to eliminate this bright area. In addition, this paper mentions turning off white light illumination during data collection, which we plan to do as well. Finally, we hope to replicate some of the accuracy tests on basic objects to validate our own 3D reconstruction, in particular the skin against a glass plate to replicate human tissue and the curved object to replicate a shape that may be seen during endoscopy.

## **Paper 2: Spectrally encoded fiber-based structured lighting probe for intraoperative 3D imaging**

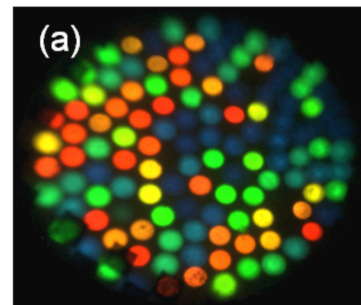
### Motivation

Reconstruction of 3D surfaces in minimally invasive surgery can improve precision by making it possible to do registration of pre-operative imaging data with the live surgery video. One effective way to do 3D reconstruction is structured light, as the light pattern can create features on otherwise featureless tissue. One typical difficulty is the identification of specific features within the pattern. This paper seeks to address this issue by design a system for 3D reconstruction that uses a laser pattern with uniquely colored spots to allow for identification.

### Technical Approach

#### *Probe Design*

Collimated laser output was sent through a prism, focused into a thin line, then sent through a linear fiber array and projection lens to produce a (fixed) random pattern of uniquely colored dots (shown to the right).



#### *Wavelength segmentation and centroiding*

First, the dominant wavelength for each pixel of interest is calculated to create a ‘ $\lambda$ -image’. For each dot in the pattern, a filter is applied to this ‘ $\lambda$ -image’ to obtain only those pixels with wavelengths near the wavelength associated with that dot. A region-growing algorithm followed by a median filter is applied to fill gaps in the dot and remove erroneous pixels. The centroid of the detected region and histogram of wavelength values in it is recorded, with the peak value in the histogram being recorded as the wavelength label for the dot.

#### *3D reconstruction*

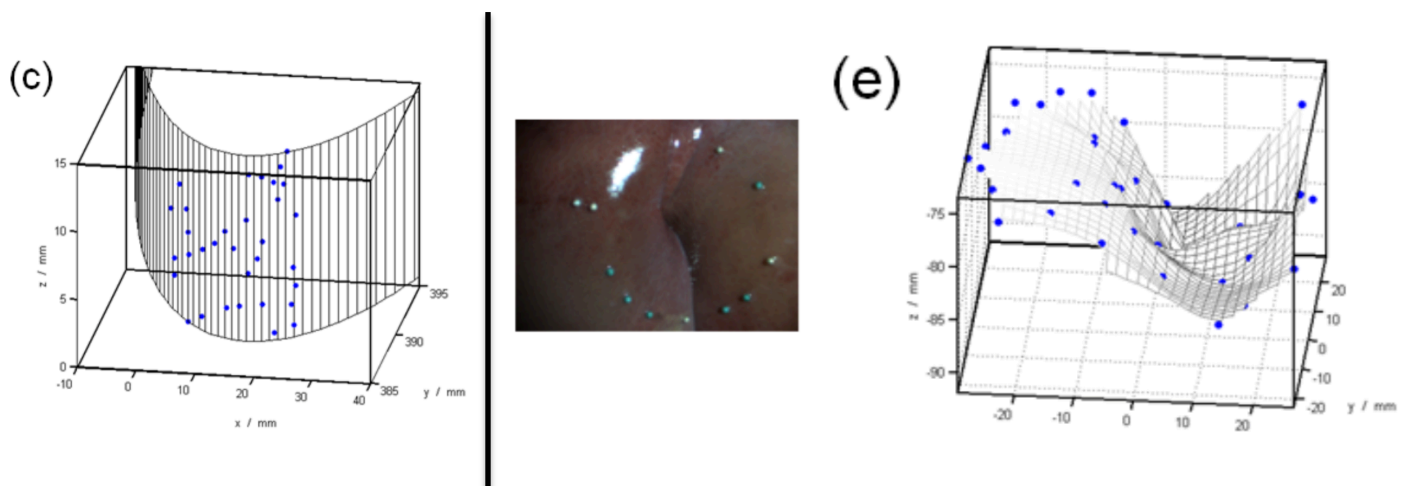
Standard calibration based on the pinhole camera model was performed with a checkerboard pattern, with an image collected with and without the laser pattern for each checkerboard position. Data with the laser pattern turned on were used to compute light rays for each spot in the pattern, giving the origin of the projector relative to the camera. Knowing these rays, any laser pattern dot in a new image could be used to create a ray through the camera pinhole and the location on the image plane of the camera. This camera ray could be intersected with the laser projector ray found from calibration to compute 3D coordinates of the feature point.

### *Characterization and ex vivo testing*

The effectiveness of the wavelength computing algorithm was tested by projecting the pattern onto a white screen and collecting images. The true spectra of individual spots were measured using an optical fiber probe placed in the pattern’s plane and connected to a spectrometer. To account for variance in optical properties of body tissue, the system was evaluated on biological tissue of varying optical properties to assess the accuracy of the computed wavelength.

### Results

In order to distinguish similar colors reliably, the algorithm used for wavelength computing required a signal in at least two of the three channels (RGB). It was also found that computed wavelength values were in general agreement with ground truth, but that there were some errors at the high and low end of the wavelength spectrum depending on the background color. For calibration, the average error of fitting projector rays to points was 0.32mm. Two opaque validation objects were used to test reconstruction, a flat black object and a brown cylinder. Reconstructions were evaluated by fitting a surface to the generated 3D point cloud using a least-squares minimization algorithm then finding the error between points and the surface and checking that dimensions matched the actual objects (results for cylinder below on left). For both objects, the algorithm provided sub-millimeter accuracy. Ex vivo tissue samples including kidney, liver, and fatty tissue were also tested to demonstrate reconstruction in a more realistic setting. These results were visually confirmed but no quantitative results were provided (results below on right for porcine liver “valley”)



### Critique

Like in the previous article, the biggest issue is the lack of quantitative results from the more realistic models, but the group mentions this in their conclusion section and has actually published a more recent paper with this type of data for an updated version of the system. In addition, although these models may be realistic in terms of tissue color, it might be more meaningful to collect images that look more similar to actual endoscopy images (like the oral cavity image from the previous paper). Another weakness was that there were a very limited number of spots in the pattern, resulting in sparse reconstructions from a single image. Data from multiple images would need to be combined to provide meaningful data. Along the same lines, the dots are quite large and thus more likely to be partially occluded which would affect centroid location and thus 3D feature location. Although not relevant to our project, they also had trouble with distinguishing dots based on wavelength for certain wavelengths on certain background colors. Again, a discussion of the runtime of the algorithm may be helpful for assessing fit into clinical workflow.

### Relevance

For our project, we plan to use the region growing algorithm followed by a median filter to create a binary image containing only the green dots. This would improve the robustness of our dot detection algorithm, which currently runs on the raw image. Also similar to this paper, we have relatively sparse data points from each image (although more dense than this paper). We plan to use the surface fitting based on a least-squares approach to approximate surfaces to fit our data points to use in evaluating the accuracy of our reconstructions.

### **References**

1. M. Chan, W. Lin, J Qu, “Miniaturized three-dimensional endoscopic imaging system based on active stereovision,” in *Applied Optics*. **42**(10), 1888-1898 (2003)
2. N. T. Clancy, D. Stoyanov, L. Maier-Hein, A. Groch, G. Yang, D. Elson, “Spectrally encoded fiber-based structured lighting probe for intraoperative 3D imaging,” in *Biomedical Optics Express*. **2**(11), 3119-3128 (2011).